Heteroatom Chemistry
Volume 11, Number 1, 2000

Ab Initio Molecular Orbital Study of Dications of 1,5-Dichalcogenacyclooctanes

Naofumi Nakayama,[1] Ohgi Takahashi,[1] Osamu Kikuchi[1], and Naomichi Furukawa[2]

[1]Department of Chemistry, University of Tsukuba, Tsukuba 305-8571, Japan

[2]Tsukuba Advanced Research Alliance Center, University of Tsukuba, Tsukuba 305-8577, Japan

Received 14 July 1999

ABSTRACT: *The molecular and electronic structures of the dications of three homonuclear and three heteronuclear dichalcogenacyclooctanes (chalcogen = S, Se, or Te) were investigated by ab initio molecular orbital calculations. Four energy-minimum structures were located for each dication. Three of those (chair-chair, boat-boat, and boat-chair) have the cis configuration with respect to the chalcogen lone pairs, and the remaining one has the trans configuration. The cis isomers were found to be much more stable than the trans isomer. Among the three cis structures, the stability is in the order of boat-chair > boat-boat > chair-chair for all dications. This order can be explained by considering the nonbonding $H\cdots H$ interactions. The chair-chair structure (C_{2v} symmetry) of the 1,5-dithiacyclooctane dication has a very low vibrational frequency of a_2 symmetry, and its LUMO energy is lower than those of boat-boat and boat-chair. These can rationalize the fact that in the crystalline state the dication adopts a distorted C_2 chair-chair conformation. The transition states between the three conformers of the homonuclear dications were also located. The corresponding energy barriers are relatively low, which is consistent with their NMR spectra. The relative stabilities of the homonuclear and heteronuclear dications were elucidated on the basis of their energies and those of the corresponding neutral compounds.* © 2000 John Wiley & Sons, Inc. Heteroatom Chem 11:31–41, 2000

INTRODUCTION

1,5-Dithiacyclooctane (1,5-DTCO, 1,5-Dithiocane, **1**) is well known in heteroatom chemistry for the unusual stability of its dication [1–3]. This stability is due to the bond formation between the two sulfur atoms (Scheme 1) and, therefore, arises from a strong transannular interaction. The dicationic species $\mathbf{1}^{2+}$ is unusual in that two cationic atoms are directly bonded to each other. $\mathbf{1}^{2+}$ is formed by electrochemical [4,5] or chemical [1,6] oxidation of **1** and by reactions of its monooxide [7,8]. Crystal structures of $\mathbf{1}^{2+}\cdot 2CF_3SO_3^-$ were determined by X-ray analysis [9], showing the S–S bond distances of about 2.1Å and distorted C_2 chair-chair structures. The solid state Raman spectra of $\mathbf{1}^{2+}$ and its deuterated analogs were presented by Tamaoki et al. [10].

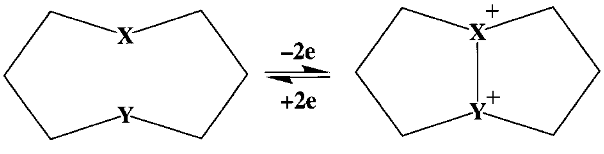

1: X=Y=S **2**: X=Y=Se **3**: X=Y=Te
4: X=S, Y=Se **5**: X=S, Y=Te **6**: X=Se, Y=Te

SCHEME 1

Correspondence to: Osamu Kikuchi, Naomichi Furukawa.

Contract Grant Sponsor: TARA Project Fund, University of Tsukuba.

They assigned the 430 cm^{-1} band of $\mathbf{1}^{2+} \cdot 2BF_4^-$ to the coupled vibration of the S^+–S^+ stretching mode and a skeletal deformation vibration, the 446 cm^{-1} band to the S^+–S^+ stretching mode, and 502, 550, 603, and 644 cm^{-1} bands to the C–S^+ stretching modes. The latter four values are lower than the values for the C–S stretching modes of the neutral **1** [11], indicating that the C–S bonds in the dication are weaker than in the neutral state.

The oxidation of **1** is electrochemically reversible [4,5]. The oxidation potential of **1** is 0.34 V under conditions in which ordinary sulfides are oxidized with peak potentials 1.2–1.7 V [4]. Of particular interest is the fact that although in dilute solutions, the oxidation of **1** corresponds to the removal of two electrons, only one oxidation peak was observed. It was shown that the removal of the second electron is easier than that of the first electron by 20 mV [5].

1,5-Diselenacyclooctane (1,5-DSeCO, 1,5-diselenocane, **2**) and 1,5-ditelluracyclooctane (1,5-DTeCO, 1,5-ditellurocane, **3**) are also very easily oxidized chemically or electrochemically and form stable dications (Scheme 1) [12–14]. In the cyclic voltammogram of **2** and **3**, the potentials of the oxidation peak are +0.25 V and −0.02 V, respectively (vs. Ag/0.01M $AgNO_3$) [13,14]. These are also remarkably low potentials compared with the corresponding monochalcogenide or other corresponding mesocyclic dichalcogenide compounds. They also show only one reversible oxidation peak although their oxidation reactions are two-electron-transfer processes.

Crystal structures of $\mathbf{2}^{2+} \cdot 2BF_4^- \cdot CH_3CN$ were also determined by X-ray analysis [15], showing the Se–Se bond distances of about 2.4 Å and a boat-chair conformation with C_1 symmetry.

The ^{1}H- and the ^{13}C-NMR spectra of $\mathbf{1}^{2+}$, $\mathbf{2}^{2+}$, and $\mathbf{3}^{2+}$ were also reported [7,8,12,14]. Their ^{1}H-NMR spectra showed a broad peak, whereas their ^{13}C-NMR spectra showed that the four carbon atoms adjacent to the chalcogen atoms are equivalent and that the other two carbon atoms are equivalent. These results indicate that a conformational change between some structures may occur in each compound.

Although $\mathbf{1}^{2+}$ is a prototype of many dichalcogenide dications [1–3,16], there are no theoretical studies on this dication except for the STO-3G calculations by Tamaoki et al. [10]. They reported only two structures (TBB and CC; see Ref. 10 for the designation of conformations). In the present study, we investigated molecular and electronic structures of $\mathbf{1}^{2+}$–$\mathbf{3}^{2+}$ by ab initio molecular orbital calculations. Also included in this article are the computational results on the dications of **4**–**6**. Although these heteronuclear dications are hitherto unknown, a dibenzo derivative of $\mathbf{4}^{2+}$ was detected [17] and a dibenzo derivative of $\mathbf{5}^{2+}$ was isolated [18]. We discuss the relative stabilities among the six dications with respect to the neutral state, and preference between homonuclear ($\mathbf{1}^{2+}$–$\mathbf{3}^{2+}$) and heteronuclear ($\mathbf{4}^{2+}$–$\mathbf{6}^{2+}$) dications.

CALCULATIONS

Calculations were performed using SPARTAN version 4.0 [19]. The RHF method was employed with the 3-21G$^{(*)}$ basis set which includes d-type polarization functions on sulfur, selenium, and tellurium atoms. The 6-31G* basis set was also used for $\mathbf{1}^{2+}$.

Four structures were considered for each dication (Figure 1): three of those [chair-chair (CC), boat-boat (BB), and boat-chair (BC)] have the cis configuration with respect to the two chalcogen lone pairs (as observed for $\mathbf{1}^{2+}$ and $\mathbf{2}^{2+}$ by X-ray crystallographic analysis [9,15]), and the remaining one (Trans) has the trans configuration. The CC, BB, BC, and Trans structures of the dications arise from the CC, BB1, BC1, and twist-chair (TC) conformers of the corresponding neutral species, respectively [20]. Geometry optimizations for $\mathbf{1}^{2+}$–$\mathbf{3}^{2+}$ were performed in C_{2v} symmetry for CC and BB, in C_s symmetry for BC, and in C_{2h} symmetry for Trans. For CC, BB, and

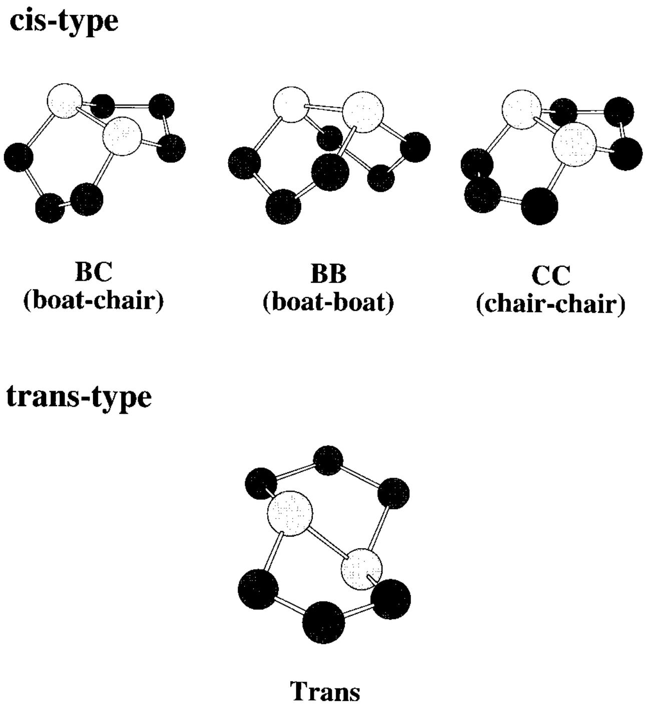

FIGURE 1 Four energy-minimum structures of $\mathbf{1}^{2+}$ obtained by RHF/6-31G* geometry optimizations.

Trans structures of **4**$^{2+}$–**6**$^{2+}$, C_s symmetry was imposed. Transition states between BC and BB (TS1) and between BC and CC (TS2) were also located for **1**$^{2+}$–**3**$^{2+}$. Vibrational frequency calculations were performed for all the stationary points located to confirm that they corresponded to a true minimum or a transition state.

The atomic charges were evaluated by the natural population analysis [21], which is more recommended than the traditional Mulliken population analysis, especially for molecules with strong polar bonds.

We also examined the triplet biradical state for **1**$^{2+}$ by the UHF/3-21G$^{(*)}$ and UHF/6-31G* methods. This species was considered as one that does not have a bond between the two sulfur atoms. Two conformations were taken into account for the triplet dication: one of the two possible twist-boat-chair conformations (TBC1) and one of the two possible boat-boat conformations (BB2) (see Ref. [20] for the designation of conformations). According to our previous ab initio study of the neutral state of **1** [20], the TBC1 conformer is the most stable among the nine conformers found and its lone-pair–lone-pair splitting is relatively small, and in the BB2 conformer there is little interaction between the two sulfur lone pairs because the two lone-pair orbitals are nearly orthogonal to each other.

RESULTS AND DISCUSSION

Energy-Minimum Structures. General Trend
For all the six compounds, the four structures (BC, BB, CC, and Trans) were calculated to be a minimum. Table 1 shows the relative energies of the four structures of each compound. Figure 1 shows the four structures of **1**$^{2+}$ obtained by 6-31G* geometry optimizations, and the calculated skeletal structural parameters of **1**$^{2+}$–**6**$^{2+}$ are presented in Tables 2–8. The numbering of the carbon atoms is shown in Figure 2.

In all compounds, the BC structure was calculated to be the most stable, and the relative energy

TABLE 1 Relative Energies (kcal mol^{-1}) of Four Structures of **1**$^{2+}$–**6**$^{2+}$ Calculated by RHF/3-21G$^{(*)}$ and RHF/6-31G* (in parentheses)

Compound	*BC*^{a}	*BB*	*CC*	*Trans*
1^{2+}	0.0	1.2	2.3	29.2
	(0.0)	(1.1)	(1.6)	(28.2)
2^{2+}	0.0	1.6	2.6	40.8
3^{2+}	0.0	1.3	1.6	47.0
4^{2+}	0.0	1.4	2.4	34.3
5^{2+}	0.0	1.2	2.2	37.1
6^{2+}	0.0	1.5	2.1	43.5

[a] The total energies (in hartrees) for the BC structures are −1023.575239 (**1**$^{2+}$ by 3-21G$^{(*)}$), −1028.554759 (**1**$^{2+}$ by 6-31G*), −5009.690380 (**2**$^{2+}$), −13398.850400 (**3**$^{2+}$), −3016.632657 (**4**$^{2+}$), −7211.216524 (**5**$^{2+}$), and −9204.272433 (**6**$^{2+}$).

TABLE 2 Selected Structural Parameters for **1**$^{2+}$ (3-21G$^{(*)}$)

Parameters	*BC*	*BB*	*CC*	*Trans*
Bond Lengths (Å)				
S-S	2.118	2.109	2.121	2.067
S-C_2	1.853	1.852	1.856	1.840
S-C_6	1.851	1.852	1.856	1.840
Bond Angles (Degrees)				
S-S-C_2	96.1	96.4	96.2	89.4
S-S-C_6	96.1	96.4	96.2	89.4
C_2-S-C_8	105.7	107.2	107.2	123.2
S-C_2-C_3	107.0	110.2	106.8	102.7
S-C_6-C_7	108.8	110.2	106.8	102.7
C_2-C_3-C_4	109.3	110.0	109.6	114.6
C_6-C_7-C_8	109.3	110.0	109.6	114.6
Dihedral Angles (Degrees)				
C_2-S-S-C_4	0.0	0.0	0.0	56.8
C_2-S-S-C_6	−106.5	−108.2	−108.1	180.0
S-S-C_2-C_3	−27.0	23.1	−27.0	−49.4
S-S-C_6-C_7	25.5	23.1	−27.0	49.4
C_8-S-C_2-C_3	−125.1	−75.6	−125.4	−138.3
C_4-S-C_6-C_7	−72.6	−75.6	−125.4	138.3
S-C_2-C_3-C_4	51.3	−42.9	51.4	22.1
S-C_6-C_7-C_8	−47.7	−42.9	51.4	−22.1

TABLE 3 Selected Structural Parameters for **1**$^{2+}$ (6-31G*)

Parameters	*BC*	*BB*	*CC*	*Trans*
Bond Lengths (Å)				
S-S	2.113	2.106	2.114	2.059
S-C_2	1.860	1.859	1.862	1.848
S-C_6	1.857	1.859	1.862	1.848
Bond Angles (Degrees)				
S-S-C_2	96.1	96.3	96.2	89.5
S-S-C_6	96.1	96.3	96.2	89.5
C_2-S-C_8	106.9	108.4	108.4	124.6
S-C_2-C_3	106.7	110.1	106.5	102.8
S-C_6-C_7	108.8	110.1	106.5	102.8
C_2-C_3-C_4	110.4	110.7	110.6	115.7
C_6-C_7-C_8	110.2	110.7	110.6	115.7
Dihedral Angles (Degrees)				
C_2-S-S-C_4	0.0	0.0	0.0	55.4
C_2-S-S-C_6	−107.8	−109.4	−109.3	180.0
S-S-C_2-C_3	−26.6	22.8	−26.6	−48.7
S-S-C_6-C_7	24.8	22.8	−26.6	48.7
C_8-S-C_2-C_3	−124.8	−76.1	−125.2	−137.7
C_4-S-C_6-C_7	−73.5	−76.1	−125.2	137.7
S-C_2-C_3-C_4	51.2	−42.6	51.3	21.7
S-C_6-C_7-C_8	−46.8	−42.6	51.3	−21.7

TABLE 4 Selected Structural Parameters for **2**$^{2+}$

Parameters	*BC*	*BB*	*CC*	*Trans*
Bond Lengths (Å)				
Se-Se	2.343	2.334	2.347	2.312
Se-C$_2$	1.986	1.982	1.989	1.983
Se-C$_6$	1.982	1.982	1.989	1.983
Bond Angles (Degrees)				
Se-Se-C$_2$	92.8	93.2	92.8	84.2
Se-Se-C$_6$	92.8	93.2	92.8	84.2
C$_2$-Se-C$_8$	100.9	103.2	102.1	120.7
Se-C$_2$-C$_3$	108.1	111.5	108.1	102.8
Se-C$_6$-C$_7$	109.7	111.5	108.1	102.8
C$_2$-C$_3$-C$_4$	111.3	112.4	111.4	117.1
C$_6$-C$_7$-C$_8$	111.4	112.4	111.4	117.1
Dihedral Angles (Degrees)				
C$_2$-Se-Se-C$_4$	0.0	0.0	0.0	58.3
C$_2$-Se-Se-C$_6$	−101.1	−103.5	−102.2	180.0
Se-Se-C$_2$-C$_3$	−27.7	23.6	−27.6	−53.3
Se-Se-C$_6$-C$_7$	26.4	23.6	−27.6	53.3
C$_8$-Se-C$_2$-C$_3$	−121.1	−70.4	−121.1	−133.1
C$_4$-Se-C$_6$-C$_7$	−67.1	−70.4	−121.1	133.1
Se-C$_2$-C$_3$-C$_4$	55.3	−45.9	55.3	25.1
Se-C$_6$-C$_7$-C$_8$	−51.9	−45.9	55.3	−25.1

TABLE 5 Selected Structural Parameters for **3**$^{2+}$

Parameters	*BC*	*BB*	*CC*	*Trans*
Bond Lengths (Å)				
Te-Te	2.768	2.759	2.769	2.725
Te-C$_2$	2.198	2.198	2.200	2.202
Te-C$_6$	2.196	2.198	2.200	2.202
Bond Angles (Degrees)				
Te-Te-C$_2$	87.5	87.8	87.6	79.4
Te-Te-C$_6$	87.5	87.8	87.6	79.4
C$_2$-Te-C$_8$	99.8	102.7	100.4	121.6
Te-C$_2$-C$_3$	110.7	113.6	110.7	105.2
Te-C$_6$-C$_7$	111.9	113.6	110.7	105.2
C$_2$-C$_3$-C$_4$	113.7	114.8	113.8	120.5
C$_6$-C$_7$-C$_8$	113.9	114.8	113.8	120.5
Dihedral Angles (Degrees)				
C$_2$-Te-Te-C$_4$	0.0	0.0	0.0	54.7
C$_2$-Te-Te-C$_6$	−99.9	−102.8	−100.5	180.0
Te-Te-C$_2$-C$_3$	−28.4	25.4	−28.3	−54.3
Te-Te-C$_6$-C$_7$	27.5	25.4	−28.3	54.3
C$_8$-Te-C$_2$-C$_3$	−115.5	−61.9	−115.4	−124.7
C$_4$-Te-C$_6$-C$_7$	−59.5	−61.9	−115.4	124.7
Te-C$_2$-C$_3$-C$_4$	60.4	−52.7	60.3	27.5
Te-C$_6$-C$_7$-C$_8$	−57.9	−52.7	60.3	−27.5

TABLE 6 Selected Structural Parameters for **4**$^{2+}$

Parameters	*BC*	*BB*	*CC*	*Trans*
Bond Lengths (Å)				
S-Se	2.237	2.229	2.240	2.194
S-C$_2$	1.857	1.851	1.860	1.840
S-C$_8$	1.850	1.851	1.860	1.840
Se-C$_4$	1.982	1.984	1.986	1.984
Se-C$_6$	1.983	1.984	1.986	1.984
Bond Angles (Degrees)				
Se-S-C$_2$	96.8	96.8	97.0	90.1
Se-S-C$_8$	96.5	96.8	97.0	90.1
S-Se-C$_4$	91.9	92.4	91.8	83.6
S-Se-C$_6$	92.1	92.4	91.8	83.6
C$_2$-S-C$_8$	105.1	107.1	106.6	124.5
C$_4$-Se-C$_6$	101.9	103.9	102.9	119.2
S-C$_2$-C$_3$	108.6	111.5	108.4	103.0
S-C$_8$-C$_7$	109.9	111.5	108.4	103.0
Se-C$_4$-C$_3$	106.3	110.2	106.4	102.6
Se-C$_6$-C$_7$	108.5	110.2	106.4	102.6
C$_2$-C$_3$-C$_4$	110.4	111.2	110.5	116.0
C$_6$-C$_7$-C$_8$	110.4	111.2	110.5	116.0
Dihedral Angles (Degrees)				
C$_2$-S-Se-C$_4$	−2.9	−2.1	−2.4	57.5
C$_2$-S-Se-C$_6$	−104.8	−106.1	−105.4	178.0
C$_8$-S-Se-C$_4$	103.3	106.1	105.4	−178.0
C$_8$-S-Se-C$_6$	1.3	2.1	2.4	−57.5
Se-S-C$_2$-C$_3$	−24.9	25.6	−25.2	−51.6
Se-S-C$_8$-C$_7$	−27.5	−25.6	25.2	51.6
S-Se-C$_4$-C$_3$	29.9	−21.4	29.5	−50.9
S-Se-C$_6$-C$_7$	24.7	21.4	−29.5	50.9
C$_8$-S-C$_2$-C$_3$	−123.5	−73.7	−124.7	−141.7
C$_2$-S-C$_8$-C$_7$	71.4	73.7	124.7	141.7
C$_6$-Se-C$_4$-C$_3$	122.4	71.7	121.7	−129.8
C$_4$-Se-C$_6$-C$_7$	−67.7	−71.7	−121.7	129.8
S-C$_2$-C$_3$-C$_4$	52.8	−46.0	52.9	21.1
S-C$_8$-C$_7$-C$_6$	51.2	46.0	−52.9	−21.1
Se-C$_4$-C$_3$-C$_2$	−54.5	43.3	−54.4	26.0
Se-C$_6$-C$_7$-C$_8$	−49.1	−43.3	54.4	−26.0

order is BC $<$ BB $<$ CC $<$ Trans. The energies of BB and CC are close to that of BC, and the Trans structure is much more unstable than any other structure in all compounds. The instability of the Trans structure increases as the atomic number of the chalcogen atoms increases.

It seems that the slight energy differences between the three cis-type structures (BC, BB, and CC) are caused by the differences in the nonbonding repulsion between hydrogen atoms. The sum of van der Waals radii of two hydrogen atoms is 2.4 Å. Figure 3 shows the distances between hydrogen atoms which are in the vicinity of 2.4 Å in the calculated three structures of **1**$^{2+}$. In BC, these distances are longer than in BB and CC.

It should be noted that in **1**$^{2+}$, the S–C bonds are longer than the corresponding bonds in **1** [20] by

TABLE 7 Selected Structural Parameters for **5**$^{2+}$

Parameters	*BC*	*BB*	*CC*	*Trans*
Bond Lengths (Å)				
S-Te	2.470	2.461	2.472	2.419
S-C_2	1.858	1.852	1.865	1.835
S-C_8	1.853	1.852	1.865	1.835
Te-C_4	2.186	2.188	2.186	2.203
Te-C_6	2.187	2.188	2.186	2.203
Bond Angles (Degrees)				
Te-S-C_2	97.1	97.0	97.2	93.7
Te-S-C_8	96.4	97.0	97.2	93.7
S-Te-C_4	85.7	86.2	85.6	75.6
S-Te-C_6	86.1	86.2	85.6	75.6
C_2-S-C_8	104.8	107.5	105.5	123.9
C_4-Te-C_6	101.1	102.5	102.9	118.8
S-C_2-C_3	110.3	113.7	110.4	104.8
S-C_8-C_7	111.8	113.7	110.4	104.8
Te-C_4-C_3	107.1	110.5	106.7	102.8
Te-C_6-C_7	109.2	110.5	106.7	102.8
C_2-C_3-C_4	112.0	113.0	112.1	117.8
C_6-C_7-C_8	112.3	113.0	112.1	117.8
Dihedral Angles (Degrees)				
C_2-S-Te-C_4	0.3	−2.9	−1.7	55.1
C_2-S-Te-C_6	−101.1	−105.8	−105.0	−179.5
C_8-S-Te-C_4	106.1	105.8	105.0	179.5
C_8-S-Te-C_6	4.7	2.9	1.7	−55.1
Te-S-C_2-C_3	−28.6	27.7	−26.6	−47.2
Te-S-C_8-C_7	−31.6	−27.7	26.6	47.2
S-Te-C_4-C_3	27.3	−21.1	29.0	−53.7
S-Te-C_6-C_7	21.7	21.1	−29.0	53.7
C_8-S-C_2-C_3	−127.2	−72.0	−126.1	−144.2
C_2-S-C_8-C_7	67.5	72.0	126.1	144.2
C_6-Te-C_4-C_3	112.4	64.2	113.5	−118.0
C_4-Te-C_6-C_7	−63.1	−64.2	−113.5	118.0
S-C_2-C_3-C_4	57.9	−50.3	57.0	9.9
S-C_8-C_7-C_6	56.2	50.3	−57.0	−9.9
Te-C_4-C_3-C_2	−55.8	45.5	−56.8	38.7
Te-C_6-C_7-C_8	−49.5	−45.5	56.8	−38.7

TABLE 8 Selected Structural Parameters for **6**$^{2+}$

Parameters	*BC*	*BB*	*CC*	*Trans*
Bond Lengths (Å)				
Se-Te	2.558	2.549	2.560	2.519
Se-C_2	1.993	1.990	1.999	1.980
Se-C_8	1.989	1.990	1.999	1.980
Te-C_4	2.190	2.189	2.190	2.203
Te-C_6	2.188	2.189	2.190	2.203
Bond Angles (Degrees)				
Te-Se-C_2	93.2	93.5	93.2	87.1
Te-Se-C_8	93.0	93.5	93.2	87.1
Se-Te-C_4	87.0	87.4	87.0	76.8
Se-Te-C_6	87.1	87.4	87.0	76.8
C_2-Se-C_8	101.0	103.9	101.5	120.2
C_4-Te-C_6	100.0	102.1	101.4	121.3
Se-C_2-C_3	110.1	113.7	110.3	104.8
Se-C_8-C_7	111.7	113.7	110.3	104.8
Te-C_4-C_3	108.4	111.4	108.2	102.9
Te-C_6-C_7	110.0	111.4	108.2	102.9
C_2-C_3-C_4	112.7	113.8	112.7	118.7
C_6-C_7-C_8	112.9	113.8	112.7	118.7
Dihedral Angles (Degrees)				
C_2-Se-Te-C_4	1.3	−1.0	−0.1	56.3
C_2-Se-Te-C_6	−98.8	−103.2	−101.7	−176.7
C_8-Se-Te-C_4	102.5	103.2	101.7	176.7
C_8-Se-Te-C_6	2.3	1.0	0.1	−56.3
Te-Se-C_2-C_3	−29.7	25.7	−28.3	−51.0
Te-Se-C_8-C_7	−29.5	−25.7	28.3	51.0
Se-Te-C_4-C_3	26.5	−23.2	27.8	−55.7
Se-Te-C_6-C_7	24.3	23.2	−27.8	55.7
C_8-Se-C_2-C_3	−123.4	−68.7	−122.2	−135.9
C_2-Se-C_8-C_7	64.3	68.7	122.2	135.9
C_6-Te-C_4-C_3	113.1	63.5	114.2	−121.1
C_4-Te-C_6-C_7	−62.1	−63.5	−114.2	121.1
Se-C_2-C_3-C_4	59.3	−50.4	58.7	16.5
Se-C_8-C_7-C_6	56.6	50.4	−58.7	−16.5
Te-C_4-C_3-C_2	−56.8	48.1	−57.5	35.6
Te-C_6-C_7-C_8	−52.9	−48.1	57.5	−35.6

0.01–0.06 Å. This agrees with the fact that in the Raman spectra of **1**$^{2+}$, the S–C streching modes show lower frequencies than in **1** [10,11]. The Se–C bond lengths in **2**$^{2+}$ are also longer than in **2** by 0.01–0.04 Å. However, there are little differences in the Te–C bond lengths between **3** and **3**$^{2+}$.

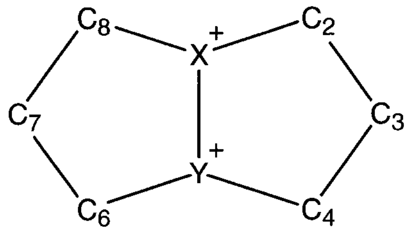

FIGURE 2 The numbering of the carbon atoms. Y is heavier than X for heteronuclear species.

Molecular Structures of **1**$^{2+}$

In the crystal structure of **1**$^{2+}$, two different C_2 structures (A, B) have been observed [9]. The S–S lengths are 2.126 and 2.122 Å for A and B, respectively. The S–C lengths are 1.842 and 1.830 Å for A, and 1.829 and 1.830 Å for B. The C–S–C angles are 104.1° and 104.6° for A and B, respectively, and the S–S–C angles are 92.7–95.9°. These experimental values are in fair agreement with the present theoretical results for the three stable structures. In the Trans structure, the S–S length and the S–S–C angles are smaller, and the C–S–C angles are larger than the others (see Tables 2 and 3).

The lowest vibrational mode of CC (41 cm^{-1} by 3-21G$^{(*)}$ and 50 cm^{-1} by 6-31G*) has a_2 symmetry

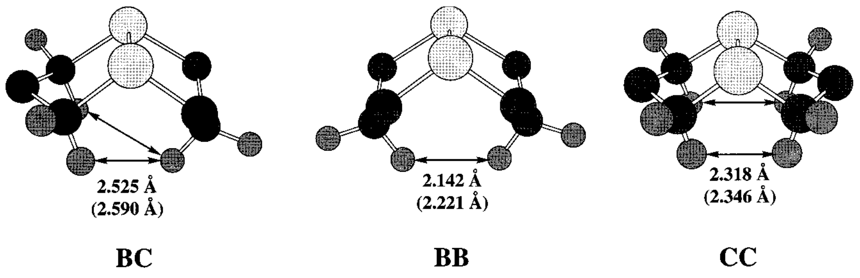

FIGURE 3 Nonbonding H···H Interactions in the BC, BB, and CC structures of $\mathbf{1}^{2+}$ calculated by 3-21G$^{(*)}$ and 6-31G* (in parentheses).

and corresponds to a ring distortion. This is consistent with the experimental result that the crystal structure is a distorted chair-chair of C_2 symmetry.

Triplet Dication of $\mathbf{1}^{2+}$

The triplet biradical state for $\mathbf{1}^{2+}$ was also investigated to a limited extent in order to see the importance of the S–S bond formation in $\mathbf{1}^{2+}$. The triplet biradical state corresponds to "two $S^{\cdot +}$ radical cations" which has no effective bond between the two S atoms. Table 9 shows that the spin density and positive charge are localized on the two S atoms in the triplet state. Table 9 also shows the calculated bond lengths, and Figure 4 shows the three structures calculated by UHF/6-31G*. These structures are not much different than the corresponding structures of the neutral state except for the S–S bond lengths (0.05–0.18 Å longer; see Table 9 and Ref. [20]), although the BB2 structures that were optimized with D_2 symmetry constraint have one imaginary frequency of b_2 symmetry (34i cm^{-1} by 3-21G$^{(*)}$, 20i cm^{-1} by 6-31G*).

The UHF/3-21G(*) or UHF/6-31G* energies of the optimized structures of the triplet $\mathbf{1}^{2+}$ are higher than the energy of the BC of the singlet state $\mathbf{1}^{2+}$ calculated by RHF/3-21G(*) or RHF/6-31G* by more than 20 kcal mol^{-1} (Table 10). Because the UHF method is expected to overestimate the stability of the triplet dication as compared with the RHF energy of the singlet dication, the actual energy difference between the singlet (S^+–S^+) and triplet dications would be larger.

Molecular Structures of $\mathbf{2}^{2+}$ *and* $\mathbf{3}^{2+}$

In the crystal structure of $\mathbf{2}^{2+}$, the Se–Se length is 2.382 Å and the Se–C lengths are 1.95–1.98 Å; the C–Se–C angles are 101.7° and 102.2°, and the Se–Se–C angles are 90.7–92.6° [14]. These experimental values are in good agreement with the present theoretical results for the three stable cis-type structures (Table 4). As in $\mathbf{1}^{2+}$, in the Trans structure the Se–Se length and the Se–Se–C angles are smaller, and the C–Se–C angles are larger than the cis-type structures. Although there are no experiments with respect to the structure of $\mathbf{3}^{2+}$, the present calculations indicate that the structural feature of $\mathbf{3}^{2+}$ is similar to that of $\mathbf{1}^{2+}$ or $\mathbf{2}^{2+}$ (see Table 5).

From Tables 2–5, the higher energies of the Trans structures can be ascribed to the distortion of the framework. Especially, the C–X–C angles of the Trans structures are much larger than those of the other structures (by 15–22°). Also, the skeletal bond angles at carbon atoms deviate significantly from the regular tetrahedral angle. These distortions are due to the poor overlap between the p_π orbitals of the two chalcogen atoms in the Trans structures. The two chalcogen atoms must approach each other in order to make the bond between them. Consequently, in the Trans structure, the X–X length and the X–X–C angles are smaller, and the C–X–C angles are larger than in the cis-type structures.

TABLE 9 Atomic Charges, Spin Densities, and Interatomic Distances of the Triplet State of $\mathbf{1}^{2+}$ Calculated by UHF/3-21G$^{(*)}$ and UHF/6-31G*[a]

Parameters	*TBC1*	*BB2* (D_2)	*BB2* (C_2)
Charges[b]			
S_1	0.997 (0.951)	1.037 (0.985)	1.036 (0.985)
S_5	1.017 (0.967)	1.037 (0.985)	1.036 (0.985)
Spin densities[b]			
S_1	1.027 (1.039)	1.025 (1.038)	1.026 (1.038)
S_5	1.028 (1.041)	1.025 (1.038)	1.026 (1.038)
Interatomic distances (Å)			
S···S	4.006 (4.087)	4.255 (4.286)	4.159 (4.245)
S_1-C_2	1.813 (1.825)	1.814 (1.826)	1.818 (1.828)
S_1-C_8	1.827 (1.837)	1.814 (1.826)	1.807 (1.822)
S_5-C_4	1.814 (1.825)	1.814 (1.826)	1.807 (1.822)
S_5-C_6	1.819 (1.829)	1.814 (1.826)	1.818 (1.828)

[a] RHF/6-31G* values in parentheses.
[b] Natural population analysis [21].

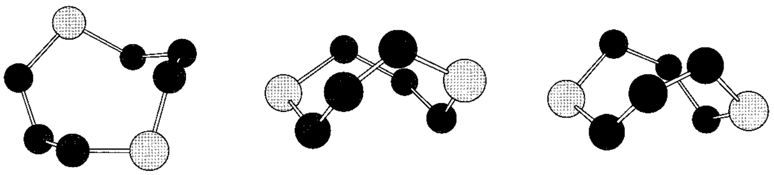

TBC1 **BB2 (D_2 symmetry)** **BB2 (C_2 symmetry)**

FIGURE 4 Three structures of the triplet state of **1**$^{2+}$ optimized by UHF/6-31G*.

TABLE 10 Relative Energies and the Numbers of Imaginary Frequencies of the Optimized Structures for the Triplet State of **1**$^{2+}$ Calculated by UHF/3-21G$^{(*)}$ and UHF/6-31G*^{a}

	TBC1	*BB2* (D_2)	*BB2* (C_2)
Relative energy^{b} (kcal mol^{-1})	22.3 (20.3)	28.7 (25.9)	28.5 (25.8)
Number of imaginary frequencies	0 (0)	1 (1)	0 (0)

[a] UHF/6-31G* values in parentheses.
[b] Relative to the most stable structure (BC) of **1**$^{2+}$.

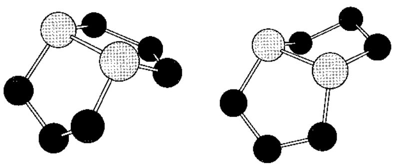

TS1 **TS2**

FIGURE 5 Two transition structures of **1**$^{2+}$ located by RHF/6-31G*.

TABLE 11 Relative Energies (kcal mol^{-1})^{a} of the Two Transition States of **1**$^{2+}$–**3**$^{2+}$ Calculated by RHF/3-21G$^{(*)}$ and RHF/6-31G*^{b}

Compound	*TS1*	*TS2*
1^{2+}	6.4 (6.2)	7.3 (6.9)
2^{2+}	7.6	9.4
3^{2+}	8.7	10.0

[a] Relative to the most stable structure (BC) of **1**$^{2+}$–**3**$^{2+}$.
[b] RHF/6-31G* values in parentheses.

Transition Structures between BC, BB, and CC in **1**$^{2+}$*,* **2**$^{2+}$*, and* **3**$^{2+}$

Figure 5 shows the two transition structures of **1**$^{2+}$ calculated by RHF/6-31G*; TS1 corresponds to the transition state between BC and BB, and TS2 corresponds to that between BC and CC. Table 11 shows the relative energies of TS1 and TS2 of **1**$^{2+}$–**3**$^{2+}$, and Tables 12–15 show their geometrical parameters. TS1 of **1**$^{2+}$ and TS2 of **1**$^{2+}$–**3**$^{2+}$ have C_1 symmetry, whereas TS1 of **2**$^{2+}$ and **3**$^{2+}$ have C_s symmetry.

From Table 11, it is expected that conformational changes occur easily between the three structures because their activation barriers are less than 10 kcal mol^{-1}. This is consistent with the ^{1}H- and ^{13}C-NMR spectra [7,8,12,14]. Interestingly, the relative energies of TS1 and TS2 are increased with increasing the atomic number of the chalcogen atoms.

Except for the TS1 of **2**$^{2+}$ and **3**$^{2+}$, the transition states do not have C_s symmetry. The C_s structures were found to have two imaginary frequencies. However, the energy differences between the C_1 and C_s structures were less than 1 kcal mol^{-1}.

*Molecular Structures of Heteronuclear Dications (***4**$^{2+}$*,* **5**$^{2+}$*, and* **6**$^{2+}$*)*

Tables 6–8 show the structural parameters of the four energy-minimum structures in **4**$^{2+}$–**6**$^{2+}$. Although there are no experiments with respect to these structures, the present calculations indicate that the structural feature is similar to **1**$^{2+}$–**3**$^{2+}$. Therefore, the instability of the Trans structures in **4**$^{2+}$–**6**$^{2+}$ is due to the reason described above for **1**$^{2+}$–**3**$^{2+}$. In **4**$^{2+}$–**6**$^{2+}$, the Y–X–C angles are larger than the X–Y–C angles in all structures (Y is heavier than X). In other words, X is drawn by Y. In view of the charge distributions, Y in **4**$^{2+}$–**6**$^{2+}$ has larger positive charge than Y in the homonuclear species, while X in **4**$^{2+}$–**6**$^{2+}$ has smaller positive charge than X in the homonuclear species (see the following section and Table 16).

Charge Distributions and LUMO Energies

Table 16 shows the positive charges of the chalcogen atoms in the dications. For the homonuclear dications, the magnitude of positive charges is increased

TABLE 12 Selected Structural Parameters for the Transition Structures of $\mathbf{1}^{2+}$ Calculated by RHF/3-21G$^{(*)}$

Parameters	*TS1*	*TS2*
Bond Lengths (Å)		
S-S	2.102	2.096
S-C$_2$	1.843	1.839
S-C$_4$	1.840	1.871
S-C$_6$	1.856	1.849
S-C$_8$	1.851	1.830
Bond Angles (Degrees)		
S-S-C$_2$	98.2	94.4
S-S-C$_8$	96.5	96.2
S-S-C$_4$	98.4	96.1
S-S-C$_6$	95.6	96.2
C$_2$-S-C$_8$	106.4	108.2
C$_4$-S-C$_6$	104.2	104.6
S-C$_2$-C$_3$	113.6	104.4
S-C$_4$-C$_3$	113.2	109.3
S-C$_6$-C$_7$	108.2	111.3
S-C$_8$-C$_7$	109.1	112.5
C$_2$-C$_3$-C$_4$	115.9	110.7
C$_6$-C$_7$-C$_8$	108.7	114.8
Dihedral Angles (Degrees)		
C$_2$-S-S-C$_4$	−7.2	23.1
C$_2$-S-S-C$_6$	−112.4	−82.3
C$_8$-S-S-C$_4$	100.5	132.0
C$_8$-S-S-C$_6$	−4.8	26.6
S-S-C$_2$-C$_3$	5.3	−44.5
S-S-C$_4$-C$_3$	8.0	2.3
S-S-C$_6$-C$_7$	30.4	−25.2
S-S-C$_8$-C$_7$	−21.4	−23.8
C$_8$-S-C$_2$-C$_3$	−94.0	−142.5
C$_6$-S-C$_4$-C$_3$	106.0	100.4
C$_4$-S-C$_6$-C$_7$	−69.8	−123.8
C$_2$-S-C$_8$-C$_7$	79.1	72.9
S-C$_2$-C$_3$-C$_4$	−0.6	53.8
S-C$_4$-C$_3$-C$_2$	−5.5	−34.5
S-C$_6$-C$_7$-C$_8$	−50.3	12.7
S-C$_8$-C$_7$-C$_6$	46.1	9.9

TABLE 13 Selected Structural Parameters for the Transition Structures of $\mathbf{1}^{2+}$ Calculated by RHF/6-31G*

Parameters	*TS1*	*TS2*
Bond Lengths (Å)		
S-S	2.100	2.095
S-C$_2$	1.854	1.849
S-C$_4$	1.852	1.875
S-C$_6$	1.861	1.858
S-C$_8$	1.856	1.842
Bond Angles (Degrees)		
S-S-C$_2$	98.0	94.8
S-S-C$_8$	96.5	96.4
S-S-C$_4$	98.2	96.1
S-S-C$_6$	95.6	96.6
C$_2$-S-C$_8$	107.6	109.4
C$_4$-S-C$_6$	105.3	105.7
S-C$_2$-C$_3$	113.5	104.3
S-C$_4$-C$_3$	113.1	108.7
S-C$_6$-C$_7$	108.3	111.5
S-C$_8$-C$_7$	109.1	112.7
C$_2$-C$_3$-C$_4$	116.6	111.3
C$_6$-C$_7$-C$_8$	109.7	115.8
Dihedral Angles (Degrees)		
C$_2$-S-S-C$_4$	−7.0	19.8
C$_2$-S-S-C$_6$	−113.4	−86.9
C$_8$-S-S-C$_4$	101.8	129.9
C$_8$-S-S-C$_6$	−4.6	23.3
S-S-C$_2$-C$_3$	5.2	−42.2
S-S-C$_4$-C$_3$	7.9	6.1
S-S-C$_6$-C$_7$	29.5	−22.6
S-S-C$_8$-C$_7$	−21.0	−20.7
C$_8$-S-C$_2$-C$_3$	−94.2	−140.7
C$_6$-S-C$_4$-C$_3$	106.0	104.7
C$_4$-S-C$_6$-C$_7$	−70.6	−120.9
C$_2$-S-C$_8$-C$_7$	79.6	76.7
S-C$_2$-C$_3$-C$_4$	−0.5	54.5
S-C$_4$-C$_3$-C$_2$	−5.6	−38.0
S-C$_6$-C$_7$-C$_8$	−49.5	11.8
S-C$_8$-C$_7$-C$_6$	45.4	8.1

with increasing the atomic number of the chalcogen atom, simply reflecting the electronegativities of the chalcogen atoms. This result indicates that the X–C bonds are more polarized as X becomes heavier.

In the heteronuclear dications, the Y atom is more positively charged than the X atom (Y is heavier than X), which indicates that the X–Y bond is polarized toward X as expected from the electronegativity difference.

Table 17 shows the LUMO energies of the four structures of each dication. In all dications, the LUMO consists mainly of the antibonding σ orbitals between the two chalcogen atoms and corresponds to the HOMO of the neutral species. Rather unexpectedly, the LUMO energies of the homonuclear dications are in the order of $\mathbf{3}^{2+} < \mathbf{1}^{2+} < \mathbf{2}^{2+}$ for all the cis-type structures. This result can not be simply explained because there are several factors to determine the LUMO energies (electronegativity, overlap between two atomic orbitals, bond length, etc.).

Although the LUMO energy is expected to be highly concerned with the reactivity as an electrophile and an oxidant, we could not see a clear relation between the LUMO energies of $\mathbf{1}^{2+}$–$\mathbf{3}^{2+}$ and their reactivities [2,22]. The effect of counteranions and/or strong electrostatic interactions associated with the high charges of dications would be needed to explain the relative reactivity.

In $\mathbf{1}^{2+}$, the CC structure has the lowest LUMO energy among the three cis-type structures. This is consistent with the fact that in the crystalline state, where counteranions interact with the sulfur atoms, $\mathbf{1}^{2+}$ has a (distorted) CC structure [9].

As expected, in the heteronuclear dications the

TABLE 14 Selected Structural Parameters for the Transition Structures of **2**$^{2+}$

Parameters	*TS1*	*TS2*
Bond Lengths (Å)		
Se-Se	2.329	2.327
Se-C$_2$	1.973	1.975
Se-C$_4$	1.973	2.001
Se-C$_6$	1.982	1.982
Se-C$_8$	1.982	1.965
Bond Angles (Degrees)		
Se-Se-C$_2$	95.2	91.0
Se-Se-C$_8$	92.8	93.6
Se-Se-C$_4$	95.2	92.9
Se-Se-C$_6$	92.8	93.3
C$_2$-Se-C$_8$	100.3	102.7
C$_4$-Se-C$_6$	100.3	99.9
Se-C$_2$-C$_3$	115.4	105.4
Se-C$_4$-C$_3$	115.4	110.4
Se-C$_6$-C$_7$	109.4	113.7
Se-C$_8$-C$_7$	109.4	114.4
C$_2$-C$_3$-C$_4$	118.8	111.9
C$_6$-C$_7$-C$_8$	110.7	118.1
Dihedral Angles (Degrees)		
C$_2$-Se-Se-C$_4$	0.0	19.4
C$_2$-Se-Se-C$_6$	−100.6	−80.7
C$_8$-Se-Se-C$_4$	100.6	122.1
C$_8$-Se-Se-C$_6$	0.0	22.0
Se-Se-C$_2$-C$_3$	−1.1	−44.2
Se-Se-C$_4$-C$_3$	1.1	7.0
Se-Se-C$_6$-C$_7$	27.0	−22.4
Se-Se-C$_8$-C$_7$	−27.0	−20.7
C$_8$-Se-C$_2$-C$_3$	−94.9	−138.1
C$_6$-Se-C$_4$-C$_3$	94.9	100.9
C$_4$-Se-C$_6$-C$_7$	−68.8	−115.9
C$_2$-Se-C$_8$-C$_7$	68.8	71.2
Se-C$_2$-C$_3$-C$_4$	2.2	59.9
Se-C$_4$-C$_3$-C$_2$	−2.2	−41.8
Se-C$_6$-C$_7$-C$_8$	−53.0	12.2
Se-C$_8$-C$_7$-C$_6$	53.0	8.7

TABLE 15 Selected Structural Parameters for the Transition Structures of **3**$^{2+}$

Parameters	*TS1*	*TS2*
Bond Lengths (Å)		
Te-Te	2.749	2.750
Te-C$_2$	2.184	2.195
Te-C$_4$	2.184	2.205
Te-C$_6$	2.194	2.193
Te-C$_8$	2.194	2.180
Bond Angles (Degrees)		
Te-Te-C$_2$	90.0	86.2
Te-Te-C$_8$	87.7	88.8
Te-Te-C$_4$	90.0	88.3
Te-Te-C$_6$	87.7	88.2
C$_2$-Te-C$_8$	99.0	103.1
C$_4$-Te-C$_6$	99.0	97.3
Te-C$_2$-C$_3$	118.7	108.3
Te-C$_4$-C$_3$	118.7	112.4
Te-C$_6$-C$_7$	111.7	117.5
Te-C$_8$-C$_7$	111.7	117.8
C$_2$-C$_3$-C$_4$	122.6	113.9
C$_6$-C$_7$-C$_8$	113.5	121.7
Dihedral Angles (Degrees)		
C$_2$-Te-Te-C$_4$	0.0	13.0
C$_2$-Te-Te-C$_6$	−99.0	−84.3
C$_8$-Te-Te-C$_4$	99.0	116.3
C$_8$-Te-Te-C$_6$	0.0	18.9
Te-Te-C$_2$-C$_3$	−0.8	−40.9
Te-Te-C$_4$-C$_3$	0.8	14.1
Te-Te-C$_6$-C$_7$	27.8	−21.1
Te-Te-C$_8$-C$_7$	−27.8	−19.5
C$_8$-Te-C$_2$-C$_3$	−88.4	−128.8
C$_6$-Te-C$_4$-C$_3$	88.4	102.1
C$_4$-Te-C$_6$-C$_7$	−61.8	−109.1
C$_2$-Te-C$_8$-C$_7$	61.8	66.3
Te-C$_2$-C$_3$-C$_4$	1.6	65.5
Te-C$_4$-C$_3$-C$_2$	−1.6	−51.1
Te-C$_6$-C$_7$-C$_8$	−58.2	12.5
Te-C$_8$-C$_7$-C$_6$	58.2	9.0

LUMO is polarized toward Y. And the LUMO energy is lower than those of the corresponding homonuclear dications for the cis-type structures. This is due to a smaller interaction between two chalcogen atomic orbitals in heteronuclear dications than in homonuclear dications.

Stability Considerations

The relative stability of the dications with respect to the neutral state can be evaluated by the energy changes of the reactions in Equation (1), where A and B are one of the bischalcogenide molecules **1**–**6**.

$$A^{2+} + B \rightarrow A + B^{2+} \qquad (1)$$

The energy change of Equation (1) is equal to $\Delta E(B \rightarrow B^{2+}) - \Delta E(A \rightarrow A^{2+})$, where $\Delta E(A \rightarrow A^{2+})$ is the

TABLE 16 The Positive Charges[a] of Chalcogen Atoms in **1**$^{2+}$–**6**$^{2+}$ Calculated by RHF/3-21G$^{(*)}$ and RHF/6-31G*[b]

Compound	*Atom*	*BC*	*BB*	*CC*	*Trans*
1^{2+}	S	0.792 (0.761)	0.794 (0.763)	0.780 (0.749)	0.773 (0.732)
2^{2+}	Se	0.889	0.894	0.876	0.858
3^{2+}	Te	1.164	1.163	1.156	1.119
4^{2+}	S	0.699	0.705	0.682	0.687
	Se	0.985	0.985	0.976	0.943
5^{2+}	S	0.513	0.516	0.492	0.508
	Te	1.471	1.472	1.469	1.391
6^{2+}	Se	0.691	0.693	0.675	0.684
	Te	1.369	1.372	1.363	1.298

[a] Natural population analysis [21].

[b] RHF/6-31G* values in parentheses.

TABLE 17 The LUMO Energies (eV) of $\mathbf{1}^{2+}$–$\mathbf{6}^{2+}$ Calculated by RHF/3-21G$^{(*)}$ and RHF/6-31G*^{a}

Compound	*BC*	*BB*	*CC*	*Trans*
$\mathbf{1}^{2+}$	−8.117 (−7.931)	−8.065 (−7.890)	−8.137 (−7.944)	−8.571 (−8.359)
$\mathbf{2}^{2+}$	−8.047	−8.000	−8.082	−8.816
$\mathbf{3}^{2+}$	−8.243	−8.304	−8.346	−9.268
$\mathbf{4}^{2+}$	−8.157	−8.116	−8.183	−8.752
$\mathbf{5}^{2+}$	−8.678	−8.640	−8.694	−9.313
$\mathbf{6}^{2+}$	−8.344	−8.297	−8.367	−9.201

^{a}RHF/6-31G* values in parentheses.

tx**TABLE 18** Energy Differences (kcal mol^{-1}) between the Neutral and Dication States of **1**–**6** Calculated by RHF/3-21G$^{(*)}$ and RHF/6-31G*^{a,b}

Compound	$\Delta E(A \rightarrow A^{2+})$
1	410.1 (410.4)
2	370.4
3	355.2
4	390.0
5	380.6
6	361.9

^{a}CC structure is postulated for both states.
^{b}RHF/6-31G* values in parentheses.

energy required to remove two electrons from A. In order to calculate these quantities, the total energies of the neutral molecules are required, and it is necessary to perform RHF/3-21G(*) calculations for **4**–**6** (the energies of **1**–**3** are available [20]). In order to estimate the relative stability of the dications from Equation (1), it is desired that the same conformation is employed for the neutral and dicationic species. Therefore, we chose the CC structure for both the neutral and dicationic states. Although the CC structures were all calculated to be higher in energy than the most stable structures for **1**–**3** [20] and $\mathbf{1}^{2+}$–$\mathbf{6}^{2+}$, the energy differences are less than 2 kcal mol^{-1}.

The $\Delta E(A \rightarrow A^{2+})$ values thus calculated are shown in Table 18. The calculated $\Delta E(A \rightarrow A^{2+})$ values are regular ones. Among the homonuclear species, the order is $\mathbf{1} > \mathbf{2} > \mathbf{3}$. This is parallel to their oxidation potentials [4,13,14]. For the heteronuclear species, the value lies between the corresponding neutral species (e.g., $\mathbf{1} > \mathbf{4} > \mathbf{2}$). We can say that the stability of the dichalcogena dications with respect to the neutral state increases in the order $\mathbf{1} < \mathbf{4} < \mathbf{5} \cong \mathbf{2} < \mathbf{6} < \mathbf{3}$.

The relative stabilities between homonuclear and heteronuclear dications can be evaluated by considering the reactions in Equations (2)–(4).

$$\mathbf{1}^{2+} + \mathbf{2}^{2+} \rightarrow \mathbf{4}^{2+} + \mathbf{4}^{2+} \qquad (2)$$

$$\mathbf{1}^{2+} + \mathbf{3}^{2+} \rightarrow \mathbf{5}^{2+} + \mathbf{5}^{2+} \qquad (3)$$

$$\mathbf{2}^{2+} + \mathbf{3}^{2+} \rightarrow \mathbf{6}^{2+} + \mathbf{6}^{2+} \qquad (4)$$

The energy changes for Equations (2)–(4) were calculated to be $+0.2$, -4.1, and -2.6 kcal mol^{-1} (calculated from the energies of BC structures; see Table 1). Therefore, there is no obvious preference for homonuclear or heteronuclear dications, although heteronuclear dications seem to be slightly preferred.

Conclusion

The present ab initio calculations showed two interesting structural features common to the homonuclear and heteronuclear dichalcogenacyclooctane dications. One is that the cis configuration with respect to the chalcogen lone pairs is much more preferred to the trans configuration. The instability of the trans configuration is caused by the poor overlap between two p_{π} orbitals of the two chalcogen atoms due to inflexibility of the ring framework. The other is that for the cis configuration the stability order is BC > BB > CC in all dications. This can be explained in part by considering nonbonding interaction between hydrogen atoms. Therefore, the crystal structure of $\mathbf{1}^{2+}$ obtained by X-ray analysis may be strongly affected by the counteranions ($CF_3SO_3^-$).

From the calculated transition state energies, interconversion among the three stable structures (BC, BB, and CC) of $\mathbf{1}^{2+}$–$\mathbf{3}^{2+}$ is expected to occur easily. This agrees well with the experimental facts from the ^{1}H- and ^{13}C-NMR spectra.

In consistency with chemical intuition, the stability order of the dications with respect to the neutral state is $\mathbf{1} < \mathbf{4} < \mathbf{5} \cong \mathbf{2} < \mathbf{6} < \mathbf{3}$. However, we found no obvious preference for homonuclear or heteronuclear dications.

REFERENCES

[1] Musker, W. K. Acc Chem Res 1980, 13, 200.
[2] Fujihara, H.; Furukawa, N. J Mol Structure (Theochem) 1989, 186, 261.
[3] Furukawa, N. Bull Chem Soc Jpn 1997, 70, 2571.
[4] Wilson, G. S.; Swanson, D. D.; Klug, J. T.; Glass, R. S.; Ryan, M. D.; Musker, W. K. J Am Chem Soc 1979, 101, 1040.
[5] Ryan, M. D.; Swanson, D. D.; Glass, R. S.; Wilson, G. S. J Phys Chem 1981, 85, 1069.
[6] Musker, W. K.; Wolford, T. L. J Am Chem Soc 1976, 98, 6745.
[7] Furukawa, N.; Kawada, A.; Kawai, T. J Chem Soc Chem Commun 1984, 1151.
[8] Fujihara, H.; Kawada, A.; Furukawa, N. J Org Chem 1987, 52, 4254.
[9] Iwasaki, F.; Toyoda, N.; Akaishi, R.; Fujihara, H.; Furukawa, N. Bull Chem Soc Jpn 1988, 61, 2563.

[10] Tamaoki, M.; Serita, M.; Shiratori, Y.; Itoh, K. J Phys Chem 1989, 93, 6052.
[11] Serita, M.; Tamaoki, M.; Itoh, K. J Phys Chem 1989, 92, 1747.
[12] Fujihara, H.; Akaishi, R.; Erata, T.; Furukawa, N. J Chem Soc Chem Commun 1989, 1789.
[13] Fujihara, H.; Akaishi, R.; Furukawa, N. Chem Lett 1990, 549.
[14] Fujihara, H.; Ninoi, T.; Akaishi, R.; Erata, T.; Furukawa, N. Tetrahedron Lett 1991, 32, 4537.
[15] Iwasaki, F.; Morimoto, M.; Yasui, M.; Akaishi, R.; Fujihara, H.; Furukawa, N. Acta Cryst 1991, C47, 1463.
[16] Glass, R. S.; Andruski, S. W.; Broeker, J. L.; Firouzabadi, H.; Steffen, L. K.; Wilson, G. S. J Am Chem Soc 1989, 111, 4036.
[17] Fujihara, H.; Mima, H.; Chiu, J-J.; Furukawa, N. Tetrahedron Lett 1990, 31, 2307.
[18] Takaguchi, Y.; Fujihara, H.; Furukawa, N. Organometallics 1996, 15, 1913.
[19] SPARTAN, version 4.0; Wavefunction, Inc.: Irvine, CA, 1995.
[20] Nakayama, N.; Takahashi, O.; Kikuchi, O.; Furukawa, N. Heteroat Chem 1999, 10, 159.
[21] Reed, A. E.; Weinstock, R. B.; Weinhold, F. J Chem Phys 1985, 83, 735.
[22] Fujihara, H.; Akaishi, R.; Furukawa, N. Tetrahedron 1993, 26, 1605.